

Exchange-energy renormalization for electrons in nanowires with Rashba spin splitting

F. S. Gray, T. Kernreiter, M. Governale,* and U. Zülicke†

*School of Chemical and Physical Sciences and MacDiarmid Institute for Advanced Materials and Nanotechnology,
Victoria University of Wellington, PO Box 600, Wellington 6140, New Zealand*

(Dated: June 10, 2019)

The exchange-interaction contribution to the total energy of a many-particle system comprised of spin-1/2 electrons confined in a cylindrical quantum wire and subject to a Rashba-type spin splitting is calculated. We find that the exchange energy per particle can be expressed in terms of a universal scaling form. In contrast to the case of spin-1/2 electrons confined to a quantum well, where Rashba spin-orbit coupling is known to slightly *enhance* the exchange energy, exchange effects in nanowires are found to be *suppressed* due to Rashba spin splitting. Our results shed new light on the interplay of spin-orbit coupling and Coulomb interaction in quantum-confined systems that are expected to host exotic quasiparticle excitations.

PACS numbers: 81.07.Gf, 71.70.Ej, 71.70.Gm, 81.05.Ea

I. INTRODUCTION

The dimensionality of a many-particle system is a crucial determinant for how importantly interaction effects can shape its physical properties. Generally, three-dimensional (3D) bulk conductors are less drastically affected by the Coulomb interaction between charge carriers than lower-dimensional, quantum-confined structures such as quasi-2D quantum wells and quasi-1D quantum (nano-)wires.¹ This is essentially due to phase-space restrictions arising from free motion being only possible in fewer than three spatial directions. Furthermore, the exact structure of transverse bound-state wave functions shapes the density distribution of the confined charge carriers and, thus, turns out to critically influence Coulombic effects in quantum wells² and wires.³ Here we explore how another aspect of quantum-confined states, namely their intrinsic spinor structure, modifies the effect of the Coulomb interaction in nanostructured systems.

Most low-dimensional conductors are fabricated from semiconductor materials where the coupling between the spin degree of charge carriers and their orbital motion is often quite strong.⁴ As a result, quantum confinement can significantly affect spin-related properties and *vice versa*.⁵ Such effects are particularly pronounced for valence-band states (i.e., *holes*) because of their peculiar spin-3/2 character.^{5,6} In contrast, conduction-band electrons are spin-1/2 particles and generally subject to weaker spin-orbit couplings that are due to the bulk inversion asymmetry in the material's crystallographic unit cell (Dresselhaus⁷ spin splitting) or the structural inversion asymmetry present in a nanostructured systems (Rashba^{8,9} spin splitting). The multitude, and often counter-intuitive nature, of spin-orbit effects in nanostructures has become the focus of recent study, with developing an understanding of the interplay with Coulomb interactions being a key question to be addressed. Bulk-hole systems,^{10–13} quantum-well-confined holes,^{14–17} and 2D electron systems subject to Rashba spin splitting^{18–22} have been considered. The comparatively few studies of Coulomb-interaction effects in spin-orbit-coupled quasi-

1D systems^{23–26} have almost exclusively focused on effective Luttinger-liquid descriptions²⁷ and, in particular, did not investigate the effect of Rashba spin splitting on the exchange energy in quantum wires. Exploring this issue in quasi-1D systems in greater detail turns out to be of interest for two reasons. Firstly, previous results revealed that spin-orbit coupling has the opposite effect on interactions in n-type and p-type quantum wells: the exchange energy of a quasi-2D conduction-band electron system is slightly enhanced^{19,21} due to spin-orbit coupling, whereas the latter significantly suppresses the exchange energy for quasi-2D holes.¹⁷ This difference warrants more systematic investigation and, as we will see below, considering the quasi-1D case sheds new light on the different ramifications of spin-orbit coupling in interacting electron systems. Secondly, quantum wires with strong spin-orbit coupling are currently attracting great interest as possible hosts of exotic quasiparticle excitations such as Majorana²⁸ and fractional²⁹ fermions. Understanding more about interaction effects in such system is a clear necessity to enable experimental observation of the unusual quasi-particle excitations.

The remainder of this article is organised as follows. We introduce our theoretical model of a Rashba-split quantum wire in Sec. II and discuss pertinent properties of the single-particle eigenstates. The formalism for calculating the exchange energy for this system is presented in Sec. III, together with the results. Amongst these is the ability to express functional dependencies of the exchange energy per particle in terms of a universal scaling function. Our findings are summarized, and related to the existing body of knowledge, in Sec. IV. Certain mathematical details are given in Appendices.

II. THEORETICAL DESCRIPTION OF RASHBA-SPLIT NANOWIRE STATES

As our model system, we consider a cylindrical quantum wire with radius R that is defined by a hard-wall potential and is also subject to a radial electric field

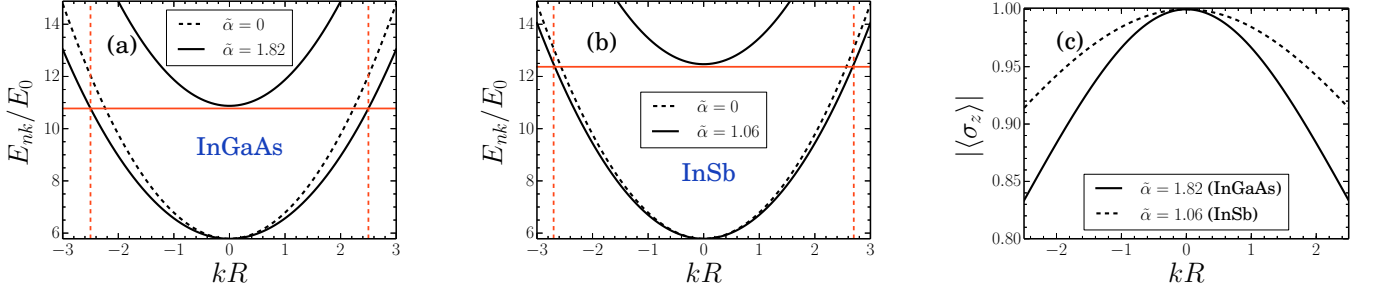


FIG. 1. Electronic structure of nanowires with Rashba spin splitting induced by a radial electric field. The solid curves in panel (a) [(b)] show the energy dispersions of the lowest two subbands obtained for a value of $\tilde{\alpha}$ corresponding to a recent experimental realization using InGaAs [InSb] as the wire material. To illustrate the effect of spin splitting, the lowest-subband dispersion for $\tilde{\alpha} = 0$ is also plotted, as the dashed curve. Vertical lines are used to indicate the range of wave numbers for which only the lowest subband is occupied. Panel (c) shows the magnitude of the expectation value for spin projection parallel to the wire axis, $|\langle \sigma_z \rangle| = \langle \sigma_z \rangle_1 = -\langle \sigma_z \rangle_2 \equiv 2 \sin^2 \eta_{kR} - 1$, for states from the lowest doubly degenerate ($n = 1$ and 2) subband.

$\mathcal{E} = \mathcal{E} \hat{\mathbf{r}}$, with constant \mathcal{E} . In a real sample, the latter could be generated, e.g., via biasing of an external gate that is wrapped around the wire surface.³⁰ For this situation of interest, the electron dynamics in the wire is described by the Hamiltonian $H = H^{(0)} + U(r)$, where

$$U(r) = \begin{cases} 0 & r < R \\ \infty & r \geq R \end{cases}, \quad (1)$$

and $H^{(0)}$ is a Rashba-type^{8,9} single-electron Hamiltonian

$$H^{(0)} = \frac{\mathbf{p}^2}{2m^*} + \frac{\alpha \mathcal{E}}{\hbar} \hat{\mathbf{r}} \cdot (\boldsymbol{\sigma} \times \mathbf{p}). \quad (2)$$

Here m^* is the band mass of electrons in the semiconductor material making up the nanowire, α is the material-dependent Rashba spin-orbit-coupling constant, and $\boldsymbol{\sigma} = (\sigma_x, \sigma_y, \sigma_z)^T$ denotes the vector of Pauli matrices. We will find the confined-electron states in the nanowire by superimposing solutions of the single-particle Schrödinger equation $H^{(0)} \psi = E \psi$ to satisfy the cylindrical hard-wall boundary condition.

The Hamiltonian (2) can be conveniently expressed in cylindrical coordinates (r, φ, z) as

$$H^{(0)} = -\frac{\hbar^2}{2m^*} \left(\frac{\partial^2}{\partial r^2} + \frac{1}{r} \frac{\partial}{\partial r} + \frac{1}{r^2} \frac{\partial^2}{\partial \varphi^2} + \frac{\partial^2}{\partial z^2} \right) \mathbb{1} + i \alpha \mathcal{E} \left[\sigma_z \frac{1}{r} \frac{\partial}{\partial \varphi} + i (e^{-i\varphi} \sigma_+ - e^{i\varphi} \sigma_-) \frac{\partial}{\partial z} \right], \quad (3)$$

where $\sigma_{\pm} = (\sigma_x \pm i \sigma_y)/2$ are the spin-1/2 ladder operators. The explicit form of (3) motivates a separation *Ansatz* for the eigenstates of $H^{(0)}$:

$$\psi(r, \varphi, z) = \frac{e^{ikz}}{\sqrt{L}} e^{i\nu\varphi} e^{-i\frac{\sigma_z}{2}\varphi} \phi_{\nu,k}(r), \quad (4)$$

where $\phi_{\nu,k}(r)$ is the radial spinor wave function, $\nu = \pm 1/2, \pm 3/2, \dots$ is an odd half-integer number, k denotes the wave number associated with the free electron motion in the quantum wire, and L is the wire length.

The resulting radial Schrödinger equation that determines $\phi_{\nu,k}(r)$ can be written in dimensionless form as $\mathcal{H}_{\nu,\kappa} \chi_{\nu,\kappa}(\varrho) = \varepsilon \chi_{\nu,\kappa}(\varrho)$, with

$$\mathcal{H}_{\nu,\kappa} = - \left(\frac{\partial^2}{\partial \varrho^2} + \frac{1}{\varrho} \frac{\partial}{\partial \varrho} \right) \mathbb{1} + \frac{\hat{m}^2}{\varrho^2} - \tilde{\alpha} \sigma_z \frac{\hat{m}}{\varrho} + \tilde{\alpha} \kappa \sigma_y + \kappa^2 \mathbb{1}, \quad (5)$$

and the definitions $\hat{m} = \nu \mathbb{1} - \frac{1}{2} \sigma_z$, $\varrho = r/R$, $\kappa = kR$, $\varepsilon = E/E_0$ where $E_0 = \hbar^2/(2m^*R^2)$, $\tilde{\alpha} = 2Rm^*\alpha\mathcal{E}/\hbar^2$, and $\phi_{\nu,k}(r) \equiv \chi_{\nu,\kappa}(r/R)$.

We employ the subband $\mathbf{k} \cdot \mathbf{p}$ method^{31,32} to find the cylindrical-nanowire eigenstates and subband-energy dispersions E_{nk} . Simultaneous invariance under time reversal ($\sigma_y \mathcal{H}_{-\nu,-\kappa}^* \sigma_y = \mathcal{H}_{\nu,\kappa}$) and spatial inversion ($e^{-i\frac{\sigma_z}{2}\varphi} \mathcal{H}_{\nu,-\kappa} e^{i\frac{\sigma_z}{2}\varphi} = \mathcal{H}_{\nu,\kappa}$) imply that each subband is (at least) doubly degenerate.³³ The first step is to find the eigenstates that are associated with the subband-edge energies E_{n0} . These states are then used as a basis set for expressing the eigenstates at general $k \neq 0$; with expansion coefficients determined from solving a matrix equation that is equivalent to the Schrödinger equation.

The Hamiltonian of Eq. (5) is diagonal when $\kappa = 0$,

$$\mathcal{H}_{\nu,0} = \begin{pmatrix} H_{\nu} & 0 \\ 0 & H_{-\nu} \end{pmatrix}, \quad (6a)$$

$$H_{\nu} = - \left(\frac{\partial^2}{\partial \varrho^2} + \frac{1}{\varrho} \frac{\partial}{\partial \varrho} \right) + \frac{(\nu - \frac{1}{2})^2}{\varrho^2} - \tilde{\alpha} \frac{\nu - \frac{1}{2}}{\varrho}, \quad (6b)$$

hence the subband-edge states are also spin-projection eigenstates of σ_z with eigenvalue $\sigma = \pm 1$. We can therefore write

$$\chi_{\nu,\kappa}(\varrho) = \sum_{n'=1}^{\infty} \left(c_{\nu,\kappa}^{(n'\uparrow)} |\nu, \uparrow, n'\rangle + c_{\nu,\kappa}^{(n'\downarrow)} |\nu, \downarrow, n'\rangle \right), \quad (7a)$$

with the subband-edge basis-state definitions

$$|\nu, \uparrow, n'\rangle = \mathcal{F}_{\nu-\frac{1}{2}}^{(\varepsilon_{\nu,+}^{(n')})}(\varrho) \begin{pmatrix} 1 \\ 0 \end{pmatrix}, \quad (7b)$$

$$|\nu, \downarrow, n'\rangle = \mathcal{F}_{-\nu-\frac{1}{2}}^{(\varepsilon_{\nu,-}^{(n')})}(\varrho) \begin{pmatrix} 0 \\ 1 \end{pmatrix}, \quad (7c)$$

and the functions $\mathcal{F}_{\sigma\nu-\frac{1}{2}}^{(\varepsilon_{\nu,\sigma}^{(n')})}(\varrho)$ being solutions of the radial-confinement problem defined by the Hamiltonian $\mathbf{H}_{\sigma\nu} + U(\varrho R)/E_0$ with corresponding dimensionless eigenenergies $\varepsilon_{\nu,\sigma}^{(n')}$. We number the subband-edge states for fixed

ν and σ in ascending order of energy, that is $\varepsilon_{\nu,\sigma}^{(n')} > \varepsilon_{\nu,\sigma}^{(n')}$ when $n' > n''$. Time-reversal symmetry mandates the Kramers degeneracy $\varepsilon_{\nu,\sigma}^{(n')} = \varepsilon_{-\nu,-\sigma}^{(n')}$. See Appendix A for more mathematical details.

The full subband dispersions can be found from solving the eigenvalue problem

$$\begin{pmatrix} \varepsilon_{\nu,+}^{(1)} + \kappa^2 & -i\tilde{\alpha}\kappa I_{\nu}^{(11)} & \dots & 0 & -i\tilde{\alpha}\kappa I_{\nu}^{(1n')} & \dots \\ i\tilde{\alpha}\kappa [I_{\nu}^{(11)}]^* & \varepsilon_{\nu,-}^{(1)} + \kappa^2 & \dots & i\tilde{\alpha}\kappa [I_{\nu}^{(1n')}]^* & 0 & \dots \\ \vdots & \vdots & \ddots & \vdots & \vdots & \ddots \\ 0 & -i\tilde{\alpha}\kappa I_{\nu}^{(1n')} & \dots & \varepsilon_{\nu,+}^{(n')} + \kappa^2 & -i\tilde{\alpha}\kappa I_{\nu}^{(n'n')} & \dots \\ i\tilde{\alpha}\kappa [I_{\nu}^{(1n')}]^* & 0 & \dots & i\tilde{\alpha}\kappa [I_{\nu}^{(n'n')}]^* & \varepsilon_{\nu,-}^{(n')} + \kappa^2 & \dots \\ \vdots & \vdots & \ddots & \vdots & \vdots & \ddots \end{pmatrix} \begin{pmatrix} c_{\nu,\kappa}^{(1\uparrow)} \\ c_{\nu,\kappa}^{(1\downarrow)} \\ \vdots \\ c_{\nu,\kappa}^{(n'\uparrow)} \\ c_{\nu,\kappa}^{(n'\downarrow)} \\ \vdots \end{pmatrix} = \varepsilon_{\nu}(\kappa) \begin{pmatrix} c_{\nu,\kappa}^{(1\uparrow)} \\ c_{\nu,\kappa}^{(1\downarrow)} \\ \vdots \\ c_{\nu,\kappa}^{(n'\uparrow)} \\ c_{\nu,\kappa}^{(n'\downarrow)} \\ \vdots \end{pmatrix}, \quad (8a)$$

with matrix elements

$$I_{\nu}^{(nn')} = 2\pi \int_0^1 d\varrho \varrho \left[\mathcal{F}_{\nu-\frac{1}{2}}^{(\varepsilon_{\nu,+}^{(n)})}(\varrho) \right]^* \mathcal{F}_{-\nu-\frac{1}{2}}^{(\varepsilon_{\nu,-}^{(n')})}(\varrho) \quad . \quad (8b)$$

For the purpose of this study, we only need to obtain the dispersion of the lowest nanowire subband. We find that, for realistic values of $\tilde{\alpha}$ (see for instance the examples below), truncation of the eigenvalue problem (8a) to the subspace spanned by the states $\{|1/2, \uparrow, 1\rangle, |1/2, \downarrow, 1\rangle\}$ and its time-reversed counterpart yields sufficiently accurate results. Hence, in the following, we will use the wave functions

$$\psi_1(r, \varphi, z) = \frac{e^{ikz}}{\sqrt{L}} \left(-i \sin \eta_{kR} |1/2, \uparrow, 1\rangle + e^{i\varphi} \cos \eta_{kR} |1/2, \downarrow, 1\rangle \right), \quad (9a)$$

$$\psi_2(r, \varphi, z) = \frac{e^{ikz}}{\sqrt{L}} \left(-i \sin \eta_{kR} |-1/2, \downarrow, 1\rangle + e^{-i\varphi} \cos \eta_{kR} |-1/2, \uparrow, 1\rangle \right) \quad (9b)$$

to describe lowest-subband states with the dispersion

$$E_{1k} \equiv E_{2k} = E_0 \left[(kR)^2 + \frac{1}{2} \left(\varepsilon_{1/2,+}^{(1)} + \varepsilon_{1/2,-}^{(1)} \right) - \frac{1}{2} \sqrt{\left(\varepsilon_{1/2,+}^{(1)} - \varepsilon_{1/2,-}^{(1)} \right)^2 + \left(2\tilde{\alpha}\kappa I_{1/2}^{(11)} \right)^2} \right]. \quad (10)$$

The coefficients entering Eqs. (9) are

$$\sin \eta_{\kappa} = \frac{1}{\sqrt{2}} \left(1 + \frac{|\varepsilon_{1/2,+}^{(1)} - \varepsilon_{1/2,-}^{(1)}|}{\sqrt{\left(\varepsilon_{1/2,+}^{(1)} - \varepsilon_{1/2,-}^{(1)} \right)^2 + \left(2\tilde{\alpha}\kappa I_{1/2}^{(11)} \right)^2}} \right)^{\frac{1}{2}}, \quad (11a)$$

$$\cos \eta_{\kappa} = \frac{1}{\sqrt{2}} \left(1 - \frac{|\varepsilon_{1/2,+}^{(1)} - \varepsilon_{1/2,-}^{(1)}|}{\sqrt{\left(\varepsilon_{1/2,+}^{(1)} - \varepsilon_{1/2,-}^{(1)} \right)^2 + \left(2\tilde{\alpha}\kappa I_{1/2}^{(11)} \right)^2}} \right)^{\frac{1}{2}}, \quad (11b)$$

Figure 1 illustrates the band structure of nanowires using parameters relevant to recent experimental realisations in Ref. 34 (InGaAs material with conduction-band effective mass $m^* = 0.037 m_0$, where m_0 is the electron mass in vacuum, $R = 300$ nm, and $\alpha \mathcal{E} = 10^{-11}$ eV m),

TABLE I. Properties of the three lowest doubly degenerate nanowire subband edges obtained for parameters applicable to recent experimental realizations.

subband index n	E_{n0}/E_0 for $\tilde{\alpha} = 1.82$	E_{n0}/E_0 for $\tilde{\alpha} = 1.06$	subband-edge (basis) state
1	5.783	5.783	$ +\frac{1}{2}, \uparrow, 1\rangle$
2	5.783	5.783	$ -\frac{1}{2}, \downarrow, 1\rangle$
3	10.87	12.47	$ +\frac{3}{2}, \uparrow, 1\rangle$
4	10.87	12.47	$ -\frac{3}{2}, \downarrow, 1\rangle$
5	18.35	16.85	$ -\frac{1}{2}, \uparrow, 1\rangle$
6	18.35	16.85	$ +\frac{1}{2}, \downarrow, 1\rangle$

and Ref. 35 (InSb, $m^* = 0.013 m_0$, $R = 50$ nm, $\alpha \mathcal{E} = 10^{-10}$ eV m). Within our model, the relevant quantity determining the effect of spin-orbit coupling is $\tilde{\alpha}$, which is equal to 1.82 and 1.06 for the InGaAs and InSb nanowires, respectively. For comparison, we show also the result for $\tilde{\alpha} = 0$. As the lowest subband-edge states have quantum numbers $\{\nu = 1/2, \uparrow\}$ and $\{\nu = -1/2, \downarrow\}$, respectively, their energy is independent of $\tilde{\alpha}$, and the spin-orbit coupling only affects the dispersion at finite k . In panel (c) of Fig. 1, we show the magnitude of the expectation value of the spin projection along the wire axis for the lowest subband as a function of the wave number k . It decreases with increasing k , as the states given in Eqs. (9) together with (11) become superposition of \uparrow and \downarrow states for finite k . Table I summarizes properties of the three lowest doubly degenerate subband edges in the two material systems.

III. EFFECT OF RASHBA SPIN SPLITTING ON THE COULOMB-EXCHANGE ENERGY

We consider the exchange energy per particle for the nanowire-electron system given by¹

$$\frac{E_X}{N} = -\frac{1}{2\rho} \sum_{n,n'} \int \frac{dk}{2\pi} \int \frac{dk'}{2\pi} V_{kk'}^{(nn')} n_F(E_{n'k'}) n_F(E_{nk}), \quad (12a)$$

where $\rho = N/L$ is the quasi-one-dimensional electron density, $n_F(E)$ denotes the Fermi-Dirac distribution function, and $V_{kk'}^{(nn')}$ is the matrix element of Coulomb inter-

action between nanowire-electron states given by

$$V_{kk'}^{(nn')} = C \int d^2 r_{\perp} \int d^2 r'_{\perp} \int_{-L/2}^{L/2} dz \frac{e^{i(k'-k)z}}{\sqrt{z^2 + |\mathbf{r}_{\perp} - \mathbf{r}'_{\perp}|^2}} \times \xi_{n'k'}^{\dagger}(\mathbf{r}_{\perp}) \xi_{nk}(\mathbf{r}_{\perp}) \xi_{nk}^{\dagger}(\mathbf{r}'_{\perp}) \xi_{n'k'}(\mathbf{r}'_{\perp}). \quad (12b)$$

Here $C \equiv e^2/(4\pi\epsilon_0\epsilon_r)$ is the Coulomb-interaction strength, $\mathbf{r}_{\perp} \equiv (r, \varphi)$ denotes the position vector in the coordinates perpendicular to the wire axis, and $\xi_{nk}(\mathbf{r}_{\perp}) \equiv e^{i\nu\varphi} e^{-i\frac{\sigma_x}{2}\varphi} \phi_{\nu,k}(r)$ is the transverse spinor part of the wavefunction in Eq. (4) for subband n . In the following, we consider the zero-temperature limit and thus replace $n_F(E) \equiv \Theta(E_F - E)$, with $\Theta(E)$ being the Heaviside step function and E_F denoting the Fermi energy. The condition $E_{nk} \equiv E_F$ defines the Fermi wave vectors k_{Fn} for occupied nanowire subbands.

We now focus on the low-density situation where only states in the lowest doubly degenerate subband are occupied up to the Fermi wave vector $k_F = k_{F1} \equiv k_{F2}$. For this situation, we can write

$$\frac{E_X}{N} = -\frac{C}{2R} [\Lambda_{\text{intra}}(\tilde{\alpha}, k_F R) + \Lambda_{\text{inter}}(\tilde{\alpha}, k_F R)], \quad (13a)$$

where Λ_{intra} (Λ_{inter}) subsumes contributions arising from the exchange interaction between particles from the same band (from different bands), given by terms with $n = n' \in \{1, 2\}$ ($n \neq n' \in \{1, 2\}$) in Eq. (12a). In the limit $L \rightarrow \infty$, we obtain the explicit expressions

$$\Lambda_{\text{intra}}(\tilde{\alpha}, \kappa_F) = \frac{1}{\kappa_F} \int_{-\kappa_F}^{\kappa_F} d\kappa \int_{-\kappa_F}^{\kappa_F} d\kappa' \int_0^1 d\varrho \varrho \int_0^1 d\varrho' \varrho' \int_0^{2\pi} d\tilde{\varphi} K_0 \left(|\kappa - \kappa'| \sqrt{\varrho^2 + \varrho'^2 - 2\varrho\varrho' \cos \tilde{\varphi}} \right) \times \left[\sin^2 \eta_{\kappa} \sin^2 \eta_{\kappa'} \left| \mathcal{F}_0^{(\epsilon_{1/2,+}^{(1)})}(\varrho) \right|^2 \left| \mathcal{F}_0^{(\epsilon_{1/2,+}^{(1)})}(\varrho') \right|^2 + \cos^2 \eta_{\kappa} \cos^2 \eta_{\kappa'} \left| \mathcal{F}_{-1}^{(\epsilon_{1/2,-}^{(1)})}(\varrho) \right|^2 \left| \mathcal{F}_{-1}^{(\epsilon_{1/2,-}^{(1)})}(\varrho') \right|^2 + \sin \alpha_{\kappa} \cos \alpha_{\kappa} \sin \alpha_{\kappa'} \cos \alpha_{\kappa'} \left(\left| \mathcal{F}_0^{(\epsilon_{1/2,+}^{(1)})}(\varrho) \right|^2 \left| \mathcal{F}_{-1}^{(\epsilon_{1/2,-}^{(1)})}(\varrho') \right|^2 + \left| \mathcal{F}_0^{(\epsilon_{1/2,+}^{(1)})}(\varrho') \right|^2 \left| \mathcal{F}_{-1}^{(\epsilon_{1/2,-}^{(1)})}(\varrho) \right|^2 \right) \right], \quad (13b)$$

$$\Lambda_{\text{inter}}(\tilde{\alpha}, \kappa_F) = \frac{1}{\kappa_F} \int_{-\kappa_F}^{\kappa_F} d\kappa \int_{-\kappa_F}^{\kappa_F} d\kappa' \sin^2(\eta_{\kappa} - \eta_{\kappa'}) \int_0^1 d\varrho \varrho \int_0^1 d\varrho' \varrho' \int_0^{2\pi} d\tilde{\varphi} \cos \tilde{\varphi} \times K_0 \left(|\kappa - \kappa'| \sqrt{\varrho^2 + \varrho'^2 - 2\varrho\varrho' \cos \tilde{\varphi}} \right) \mathcal{F}_0^{(\epsilon_{1/2,+}^{(1)})}(\varrho) \mathcal{F}_{-1}^{(\epsilon_{1/2,-}^{(1)})}(\varrho) \mathcal{F}_0^{(\epsilon_{1/2,+}^{(1)})}(\varrho') \mathcal{F}_{-1}^{(\epsilon_{1/2,-}^{(1)})}(\varrho'), \quad (13c)$$

where K_0 is the modified Bessel function of the second kind.³⁶

For the numerical evaluation of the intra-band contribution (13b), we employ a modified quadrature method,³⁷ described in greater detail in Appendix B, to deal with the logarithmic singularity encountered when the argument of $K_0(\cdot)$ approaches zero. Figure 2 illustrates the functional dependences and relative magni-

tudes of Λ_{intra} and Λ_{inter} . As can be seen, the intra-band contribution is generally dominant and weakly dependent on $\tilde{\alpha}$ values considered here. In contrast, the inter-band contribution changes quite significantly as a function of $\tilde{\alpha}$.

For quantum wires without spin splitting, i.e., in the case $\tilde{\alpha} = 0$, the exchange energy per particle was found to obey a universal scaling form.^{3,38,39} Our expression

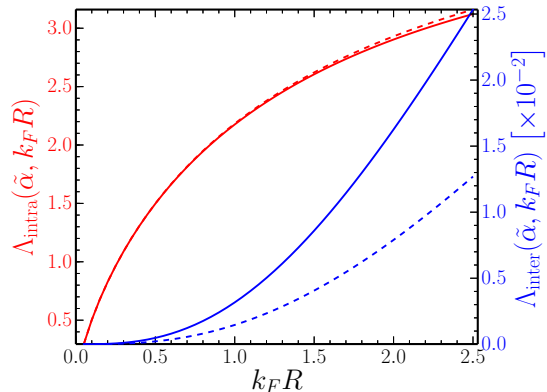


FIG. 2. Scaling functions Λ_{intra} and Λ_{inter} associated with the intra-band and inter-band contributions to the exchange energy per particle in cylindrical nanowires with spin-orbit coupling (note the scale of 10^{-2} for the inter-band contribution) See Eqs. (13a-c) for their definition. Dashed (solid) curves corresponds to $\tilde{\alpha} = 1.06$ (1.82).

for E_X/N given in Eq. (13a) generalizes these previous results to the case where spin-orbit coupling is finite. The change in magnitude of the exchange energy arising from finite $\tilde{\alpha}$ can be quantified through the relative difference

$$\Delta_X = \frac{E_X(\tilde{\alpha} \neq 0)}{E_X(\tilde{\alpha} = 0)} - 1 \quad , \quad (14)$$

which is visualized in Fig. 3. For the values of $\tilde{\alpha}$ that correspond to recent experimental realizations using InGaAs³⁴ and InSb,³⁵ the associated change amounts to a *suppression* of the exchange-energy magnitude which can be up to 1.6%. This behavior is markedly different from the case of a 2D electron system where Rashba spin

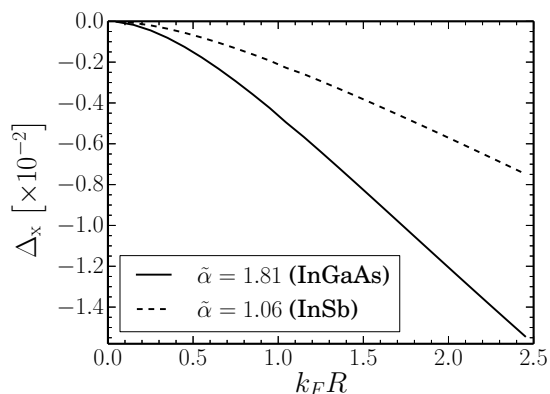


FIG. 3. Relative change Δ_X in the magnitude of the exchange energy resulting from a finite Rashba-type spin-orbit coupling quantified by parameter $\tilde{\alpha}$, as defined in Eq. (14). Note the scale factor of 10^{-2} for the abscissa. The dashed (solid) curve shows the result obtained for $\tilde{\alpha} = 1.06$ (1.82), which corresponds to a recent experimental realization using InSb (InGaAs) as the wire material.

splitting has been shown²⁰ to result in an *increase* of the exchange energy that is roughly one order of magnitude smaller. Thus the Rashba-spin-split nanowire system is more similar to a 2D hole system where the interplay between quantum confinement and spin-orbit effects also results in a suppression of the exchange energy.¹⁷

IV. CONCLUSIONS

We have studied theoretically the electronic properties of the quasi-1D electron system realized in a cylindrical quantum wire subject to a radially symmetric Rashba-type spin splitting. We determined the single-particle states for a hard-wall confinement using subband $\mathbf{k} \cdot \mathbf{p}$ theory. Focusing on the situation where only the lowest quasi-1D subband is occupied, we observed that the corresponding energy dispersion can be very accurately (to within 0.5% error) calculated from an effective 2×2 Hamiltonian. Taking the material parameters of two experimentally studied nanowire systems (one based on InGaAs and the other on InSb) as input, we have determined the influence of the Rashba spin-orbit parameter on the lowest quasi-1D subband's energy dispersion and on the spin projection of its corresponding eigenstates parallel to the wire axis, finding both quantities to be affected by an up-to 10-15% change due to the presence of spin splitting.

With single-particle states in hand, we calculated the Coulomb-exchange energy for the Rashba-spin-split quasi-1D electron system. We find that the exchange energy is *reduced* by up to 1.6%. This suppression arises from the nontrivial mixing of spin-up and spin-down components in nanowire bound states due to the presence of spin-orbit coupling, as well as the changes induced in these states' transverse density profile. Comparing the effect of spin-orbit coupling on exchange effects in quasi-1D systems with other systems, e.g., in higher dimensions, we note the qualitative difference to a 2D electron gas where the presence of Rashba spin-orbit coupling gives rise to a very slightly *enhanced* magnitude of the exchange energy.²⁰ In contrast, the confinement-induced mixing of heavy-hole and light-hole components in a quasi-2D hole system was found to suppress exchange effects,¹⁷ similar to the present case of a quasi-1D conduction-electron system. While we have focused on a specific configuration of confinement and spin-orbit coupling, our general results and overall conclusions can be expected to apply also to other spin-orbit-coupled nanowire systems, e.g., the one considered in Ref. 40.

Appendix A: Solution of the radial-confinement problem

The general solution of the differential equations present in the diagonal entries of Eq. (5) are power series,

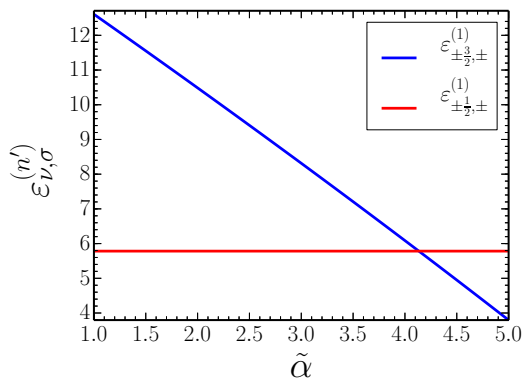


FIG. 4. Energy eigenvalues of the lowest two doubly degenerate quasi-1D subband edges, plotted as a function of the effective Rashba spin-orbit-coupling parameter $\tilde{\alpha}$.

given by,

$$\mathcal{F}_m^{(\varepsilon_{\nu,\pm}^{(n')})}(\varrho) = \varrho^m (a_0 + a_1 \varrho + \sum_{n=2}^{\infty} a_n \varrho^n) \quad (\text{A1})$$

which fulfill the relation $\mathcal{F}_{-m}^{(\varepsilon_{\nu,\pm}^{(n')})}(\varrho) = \mathcal{F}_{+m}^{(\varepsilon_{\nu,\mp}^{(n')})}(\varrho)$ yielding the eigenstates. Disregarding the ill-behaved and unphysical part in the expansion at the origin, the coefficients of the polynomials are determined by the recursion relation

$$n(n \pm 2m)a_n + m\tilde{\alpha}a_{n-1} + \varepsilon_{\nu,\pm}^{(n')}a_{n-2} = 0, \quad (\text{A2})$$

with $a_1 = -\tilde{\alpha}m/(1 \pm 2m)a_0$, where the upper (lower) sign applies to $m > 0$ ($m < 0$). The coefficient a_0 is determined by the normalisation condition $2\pi R^2 \int_0^1 \varrho |\mathcal{F}_m^{(\varepsilon_{\nu,\pm}^{(n')})}(\varrho)|^2 d\varrho = 1$. We note that the polynomial with coefficients given by Eq. (A2) represents a modified Laguerre function that becomes the standard Bessel function $J_0(\sqrt{\varepsilon_{\nu,\pm}^{(n')}}\varrho)$ for $\tilde{\alpha} = 0$ and/or $m = 0$.

The band-edge energies, $\varepsilon_{\nu,\pm}^{(n')}$ are found by imposing hard wall boundary conditions on the radial wave function, i.e. for $r = R$, we require

$$\mathcal{F}_m^{(\varepsilon_{\nu,\pm}^{(n')})}(\varrho = 1) = 0. \quad (\text{A3})$$

For not too large values of $\tilde{\alpha}$, the lowest spin- \uparrow (\downarrow) subband-edge state has $\nu = 1/2$ ($-1/2$) total angular momentum. However, as seen from Fig. 4, a level crossing occurs for $\tilde{\alpha} \approx 4.2$, beyond which the new lowest spin- \uparrow (\downarrow) subband edge is a state with $\nu = 3/2$ ($-3/2$).

Appendix B: Regularisation of the integrand for calculating the exchange energy

In the calculation of the exchange energy we have to deal with integrals of the form

$$\mathcal{I} = \iint dk dk' G(k, k') K_0 \left(|k - k'| \sqrt{r^2 + r'^2 - 2rr' \cos \varphi} \right), \quad (\text{B1})$$

with $G(k, k')$ being a smooth function of k and k' . A logarithmic singularity occurs when the argument of $K_0(\cdot)$ vanishes. This happens when either the square root is zero, at $\vec{r}_{\perp} = \vec{r}'_{\perp}$, or when $k = k'$. To regularise the integral for the case where $\vec{r}_{\perp} = \vec{r}'_{\perp}$, we add a small amount 0^+ to the term under the square root. Then by decreasing the value of 0^+ , we perform a series of calculations until the result for the exchange energy doesn't change within a certain tolerance.

The situation for $k = k'$ can be regularised analytically. To this end, we add to and subtract from Eq. (B1) the term

$$\iint dk dk' G(k, k) \ln \left(|k - k'| \sqrt{r^2 + r'^2 - 2rr' \cos \varphi + 0^+} \right). \quad (\text{B2})$$

Adding this term to Eq. (B1) cancels the logarithmic singularity. The k' -integration of the subtracted term can be performed analytically and Eq. (B1) becomes

$$\mathcal{I} = \int dk \left\{ \left[\int dk' G(k, k') K_0 \left(|k - k'| \sqrt{r^2 + r'^2 - 2rr' \cos \varphi} \right) + G(k, k) \ln \left(|k - k'| \sqrt{r^2 + r'^2 - 2rr' \cos \varphi + 0^+} \right) \right] - G(k, k) \left[k \ln \left(\frac{k_F + k}{k_F - k} \right) - 2k_F + 2k \ln \left(\sqrt{k_F^2 - k^2} \sqrt{r^2 + r'^2 - 2rr' \cos \varphi + 0^+} \right) \right] \right\}. \quad (\text{B3})$$

The expression Eq. (B3) is manifestly finite for $k = k'$.

* michele.governale@vuw.ac.nz

† uli.zuelicke@vuw.ac.nz

- ¹ G. Giuliani and G. Vignale, *Quantum Theory of the Electron Liquid* (Cambridge University Press, Cambridge, UK, 2005).
- ² T. Ando, A. B. Fowler, and F. Stern, *Rev. Mod. Phys.* **54**, 437 (1982).
- ³ A. Gold and A. Ghazali, *Phys. Rev. B* **41**, 8318 (1990).
- ⁴ P. Y. Yu and M. Cardona, *Fundamentals of Semiconductors*, 4th ed. (Springer, Berlin, 2010).
- ⁵ R. Winkler, *Spin-Orbit Coupling Effects in Two-Dimensional Electron and Hole Systems* (Springer, Berlin, 2003).
- ⁶ R. Winkler, *Phys. Rev. B* **71**, 113307 (2005).
- ⁷ G. Dresselhaus, *Phys. Rev.* **100**, 580 (1955).
- ⁸ E. I. Rashba, *Fiz. Tverd. Tela (Leningrad)* **2**, 1224 (1960), [*Sov. Phys. Solid State* **2**, 1109 (1960)].
- ⁹ Y. A. Bychkov and E. Rashba, *JETP Lett.* **39**, 78 (1984).
- ¹⁰ M. Combescot and P. Nozières, *J. Phys. C: Solid State Phys.* **5**, 2369 (1972).
- ¹¹ J. Schliemann, *Phys. Rev. B* **74**, 045214 (2006).
- ¹² J. Schliemann, *Phys. Rev. B* **84**, 155201 (2011).
- ¹³ F. V. Kyrychenko and C. A. Ullrich, *Phys. Rev. B* **83**, 205206 (2011).
- ¹⁴ W. O. G. Schmitt, *Phys. Rev. B* **50**, 15221 (1994).
- ¹⁵ S.-J. Cheng and R. R. Gerhardts, *Phys. Rev. B* **63**, 035314 (2001).
- ¹⁶ A. Scholz, T. Dollinger, P. Wenk, K. Richter, and J. Schliemann, *Phys. Rev. B* **87**, 085321 (2013).
- ¹⁷ T. Kernreiter, M. Governale, R. Winkler, and U. Zülicke, *Phys. Rev. B* **88**, 125309 (2013).
- ¹⁸ M. Pletyukhov and V. Gritsev, *Phys. Rev. B* **74**, 045307 (2006).
- ¹⁹ S. Chesi and G. F. Giuliani, *Phys. Rev. B* **75**, 155305 (2007).
- ²⁰ S. Chesi and G. F. Giuliani, *Phys. Rev. B* **83**, 235308 (2011).
- ²¹ S. Chesi and G. F. Giuliani, *Phys. Rev. B* **83**, 235309 (2011).
- ²² A. Agarwal, S. Chesi, T. Jungwirth, J. Sinova, G. Vignale, and M. Polini, *Phys. Rev. B* **83**, 115135 (2011).
- ²³ W. Häusler, *Phys. Rev. B* **63**, 121310 (2001).
- ²⁴ V. Gritsev, G. Japaridze, M. Pletyukhov, and D. Baeriswyl, *Phys. Rev. Lett.* **94**, 137207 (2005).
- ²⁵ A. Schulz, A. De Martino, P. Ingenuoven, and R. Egger, *Phys. Rev. B* **79**, 205432 (2009).
- ²⁶ F. Maier, T. Meng, and D. Loss, *Phys. Rev. B* **90**, 155437 (2014).
- ²⁷ T. Giamarchi, *Quantum Physics in One Dimension* (Clarendon Press, Oxford, UK, 2004).
- ²⁸ J. Alicea, *Rep. Prog. Phys.* **75**, 076501 (2012).
- ²⁹ J. Klinovaja, P. Stano, and D. Loss, *Phys. Rev. Lett.* **109**, 236801 (2012).
- ³⁰ K. Storm, G. Nylund, L. Samuelson, and A. P. Micolich, *Nano Lett.* **12**, 1 (2012).
- ³¹ D. A. Broido and L. J. Sham, *Phys. Rev. B* **31**, 888 (1985).
- ³² S.-R. E. Yang, D. A. Broido, and L. J. Sham, *Phys. Rev. B* **32**, 6630 (1985).
- ³³ U. Rössler, *Solid-State Theory: An Introduction*, 2nd ed. (Springer, Berlin, 2009) pp. 128-129.
- ³⁴ T. Schäpers, J. Knobbe, and V. A. Guzenko, *Phys. Rev. B* **69**, 235323 (2004).
- ³⁵ I. van Weperen, B. Tarasinski, D. Eeltink, V. S. Pribiag, S. R. Plissard, E. P. A. M. Bakkers, L. P. Kouwenhoven, and M. Wimmer, preprint arXiv:1412.0877v1.
- ³⁶ M. Abramowitz and I. A. Stegun, *Handbook of Mathematical Functions* (Dover, New York, 1964).
- ³⁷ C. Chao and S. Chuang, *Phys. Rev. B* **43**, 6530 (1991).
- ³⁸ L. Calmels and A. Gold, *Phys. Rev. B* **52**, 10841 (1995).
- ³⁹ L. Calmels and A. Gold, *Phys. Rev. B* **56**, 1762 (1997).
- ⁴⁰ A. Bringer and T. Schäpers, *Phys. Rev. B* **83**, 115305 (2011).